JOURNAL OF MATERIALS SCIENCE 33 (1998) 77–83

On deformation twins and twin-related lamellae in TiAl

ZHE JIN, G. T. GRAY III
Materials Science and Technology Division, Los Alamos National Laboratory, MST-5, MS G755, Los Alamos, NM 87545 USA

The crystal orientation relationships and atomic arrangements across deformation twin planes and twin-related lamellar interfaces in $\langle\bar{1}\,1\,0\rangle$ projection directions in TiAl are examined crystallographically. Atomic arrangements across the true-twin plane and the true-twin-related lamellar interface are shown to be identical, while the atomic arrangements across the pseudo-twin plane and the pseudo-twin-related lamellar interface are quite different. Atom locations at the true-twin plane and the true-twin-related lamellar interface do not violate the atomic order in both crystals while those at the pseudo-twin plane or the pseudo-twin-related lamellar interface are shown to violate the atomic order. $\langle\bar{1}\,1\,0\rangle$ zone diffraction pattern simulations show that the true-twins and the true-twin-related lamellae cannot be distinguished using the $\langle\bar{1}\,1\,0\rangle$ zone diffraction patterns. Not every $\langle\bar{1}\,1\,0\rangle$ zone diffraction pattern can be utilized to distinguish between any two different twin relationships. The true-twin and the pseudo-twin can only be distinguished using $\langle 1\,0\,\bar{1}]$ zone diffraction patterns, while true-twin-related and pseudo-twin-related lamellae are distinguishable by only using $\langle\bar{1}\,1\,0]$ zone diffraction patterns.

1. Introduction

Two types of twin relationships exist in γ-TiAl: deformation twins and twin-related lamellae. Deformation twins are classified as either a true-twin or a pseudo-twin due to the anisotropy of the TiAl crystal, and twin-related lamellae are classified as true-twin-related lamellae or pseudo-twin-related lamellae. The formation mechanisms of these two types of twin relationships have been extensively studied and appear to be clearly understood [1–4]. Deformation twinning has been found to be a common deformation mode in TiAl [2, 5–10]. However, systematic comparisons between these two types of twin relationships, in their crystal orientations and atomic arrangements across the twin interfaces, has not been pursued. Therefore, unambiguous determination of each twin relationship in TiAl crystals remains an unresolved question.

In a previous paper [11], all the possible twin-related lamellar interfaces in an as-grown polysynthetically twinned (PST) TiAl crystal were experimentally determined. In the current paper, the crystallographic orientation relationships in the true-twin and the pseudo-twin are investigated and compared with the twin-related lamellae. The diffraction patterns for both deformation twins and twin-related lamellae are calculated in $\langle\bar{1}\,1\,0\rangle$ zone directions to illustrate differences between all four twin relationships in TiAl.

2. Crystal orientation relationship

γ-TiAl has the $L1_0$ tetragonal crystal structure with $c/a = 1.02$. The unit cell of the γ-TiAl crystal structure is shown in Fig. 1a, in which Ti and Al atoms alternately occupy (0 0 2) planes. Because the difference between lattice parameters **c** and **a** is only 2%, γ-TiAl can be treated as an f.c.c.-based ordered crystal structure. In γ-TiAl, there exist three Shockley partial dislocations, $\frac{1}{6}\langle 1\,1\,\bar{2}\rangle$ in a (1 1 1) plane similar to the f.c.c. crystal structure. Homogeneous glide of any one of these Shockley partials on every adjacent (1 1 1) plane can shear the γ-TiAl crystal into a twin orientation with respect to the undeformed crystal. Because of the ordered structure of γ-TiAl, the resultant twins formed by these three Shockley partials are not identical. The twin formed by the passage of either $\frac{1}{6}[1\,\bar{2}\,1]$ or $\frac{1}{6}[\bar{2}\,1\,1]$ Shockley partials has a $L1_1$ crystal structure, as shown in Fig. 1b, which is also an f.c.c.-based ordered crystal structure but differs from the γ-TiAl crystal structure. The Ti and Al atoms in Fig. 1b are alternately stacked in the $(\bar{1}\,1\,1)$ planes. The $L1_1$ crystal shown in Fig. 1b is formed by homogeneous glide of $\frac{1}{6}[1\,\bar{2}\,1]$ Shockley partial dislocations in every (1 1 1) plane of the $L1_0$ crystal shown in Fig. 1a. Because of the crystal structural changes accompanying the twinning, the Ti and Al atoms in the twinned crystal are not twin-symmetric to the same atoms in the matrix, although the lattices between them are symmetric one to another across the twin plane. A twin having this type of crystal orientation relationship with the matrix is called a pseudo-twin. The detailed atomic arrangement across a pseudo-twin plane will be presented in Section 3. Contrarily, the homogeneous glide of $\frac{1}{6}[1\,1\,\bar{2}]$ Shockley partial dislocations on every (1 1 1) plane will not change the crystal structure,

0022–2461

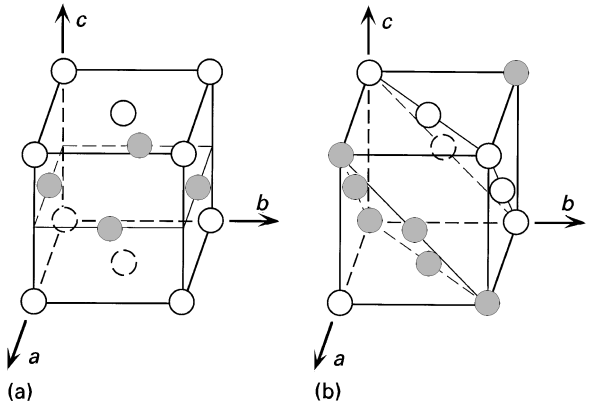

Figure 1 (a) A $L1_0$ unit cell and (b) a $L1_1$ unit cell. In (a) Ti (the shaded circles) and Al (the open circles) atoms are alternately stacked on (0 0 2) planes, while in (b) the Ti and Al atoms are alternately stacked on $(\bar{1}\,1\,1)$ planes. (b) is obtained by the motion of $\frac{1}{6}[1\,\bar{2}\,1]$ Shockley partial dislocations on every adjacent (1 1 1) plane of (a).

so the resultant twin has the same $L1_0$ crystal structure as the matrix. In this case, the twin is symmetric to the matrix both in its crystal orientations as well as its specific atomic arrangements. A twin exhibiting symmetry with the matrix in both its lattice geometry and its atomic species positions is called a true-twin [12].

Since both the true-twin and the pseudo-twin are formed by homogeneous shear in $\langle 1\,1\,\bar{2}\rangle$ directions in TiAl, the $\langle 1\,1\,\bar{2}\rangle$ twinning directions should be the same in both the matrix and the twinned crystal. Therefore, both the true-twin and the pseudo-twin have a 180°-rotational symmetry about the $\langle 1\,1\,\bar{2}\rangle$ twinning directions with respect to the matrix. The crystal orientation relationships of the true-twin and the pseudo-twin with the matrix are shown in Fig. 2a and b, respectively. The coordinates labelled with plain letters represent the crystal orientation of the matrix while those labelled with primed letters designate the orientation of the twin in Fig. 2a and b. The shaded planes in Fig. 2a and b represent the twin planes. The matrix is located below the twin plane and the twin is above the twin plane in this figure. The crystal orientation relationships between the twin and the matrix can also be seen to follow the 180°-$\langle 1\,1\,\bar{2}\rangle$ rotational symmetry in Fig. 2a and b. Although both twins satisfy the 180°-rotational symmetry about the twin plane normal [1 1 1], we use the 180°-$\langle 1\,1\,\bar{2}\rangle$ rotational symmetry to define the relative crystal orientations between the twin and the matrix since the 180°-$\langle 1\,1\,\bar{2}\rangle$ rotational symmetry reflects the twinning mechanism in TiAl.

Similar to deformation twins, two twin relationships between lamellae, a true-twin and a pseudo-twin, exist across lamellar interfaces. The formation mechanism of the twin-related lamellae however differs from that of deformation twins. In the lamellar structure, both the true-twin-related and the pseudo-twin-related lamellae are formed during the $\alpha_2 \rightarrow \gamma$ or $\alpha \rightarrow \gamma$ solid phase transformation. This is due to the specific crystal orientation relationship between the γ-TiAl phase and the α_2-Ti_3Al phase or the α-Ti_3Al phase [1, 2]. The true-twin-related lamellae (or domains) are formed when two crystals are anti-parallel in the (1 1 1) plane or 180°-rotationally symmetric about the [1 1 1] lamellar interface normal; for instance $[\bar{1}\,1\,0](1\,1\,1)$ $//[1\,\bar{1}\,0](1\,1\,1)$ [1]. For the pseudo-twin-related lamellae (or domains), two crystals are rotated relatively to one another by 60° about the [1 1 1] lamellar interface normal; for instance $[1\,\bar{1}\,0](1\,1\,1)//[\bar{1}\,0\,1](1\,1\,1)$ and $[1\,\bar{1}\,0](1\,1\,1)//[0\,1\,\bar{1}](1\,1\,1)$. Pseudo-twin-related lamellae are symmetric in their lattice geometry but not in their atomic arrangements across the lamellar interface, similar to the pseudo-twin formed during deformation. However, the pseudo-twin-related lamellae have the same $L1_0$ crystal structure, which is different from the deformation pseudo-twin.

According to the formation mechanism of twin-related lamellae in the lamellar structure, the coordinates of true-twin-related lamellae should have a 180°-[1 1 1] rotational relationship while those of the pseudo-twin-related lamellae should have a $\pm 60°$-[1 1 1] rotational relationship, respectively. The relative orientation relationships in terms of the unit cells of two twin-related lamellar laths are shown in Fig. 2c and d, in which the coordinates of the two laths are labelled by plain letters and primed letters, respectively, and the shaded triangles represent the lamellar interfaces. Because both the true-twin-related and the pseudo-twin-related lamellae are formed by relative crystal rotations about the lamellar interface normal [1 1 1], the lamellar interface index (1 1 1) should be the same with respect to both laths. In the case of deformation twins, the twin plane (1 1 1) indexed in terms of the matrix orientation should be changed to the $(\bar{1}\,\bar{1}\,\bar{1})$ twin plane when the twin plane is indexed in terms of the twin orientation since the deformation twins have a 180°-$\langle 1\,1\,\bar{2}\rangle$ rotational symmetry. Thus, the differences between deformation twins and twin-related lamellae in lamellar structures are not only due to their differences in their formation mechanisms and the crystal structural change in the pseudo-twinning but also in their orientation indexing.

3. Atomic arrangement

Since both deformation twins and twin-related lamellae display ordered superlattice structures, deformation twins and twin-related lamellae are both anisotropic in terms of their atomic arrangements, albeit the pseudo-twinning changes the $L1_0$ crystal structure into an $L1_1$ crystal structure, as shown in Fig. 2. For instance, in a (1 1 1) plane of an $L1_0$ TiAl crystal, atoms in a $[\bar{1}\,1\,0]$ direction are all like atoms, i.e. they are either all Ti atoms or all Al atoms; whereas the rows in $[0\,\bar{1}\,1]$ or $[1\,0\,\bar{1}]$ direction are alternately occupied by Ti and Al atoms. Thus, a one directional projection of these crystals cannot completely represent the atomic arrangements across the twin planes and the twin-related lamellar interfaces. Fig. 3 shows the atomic arrangements across the twin planes and the twin-related lamellar interfaces in three different $\langle \bar{1}\,1\,0\rangle$ projection directions parallel to twin planes or lamellar interfaces for each twin relationship. Circles in this figure represent the atoms in the corresponding

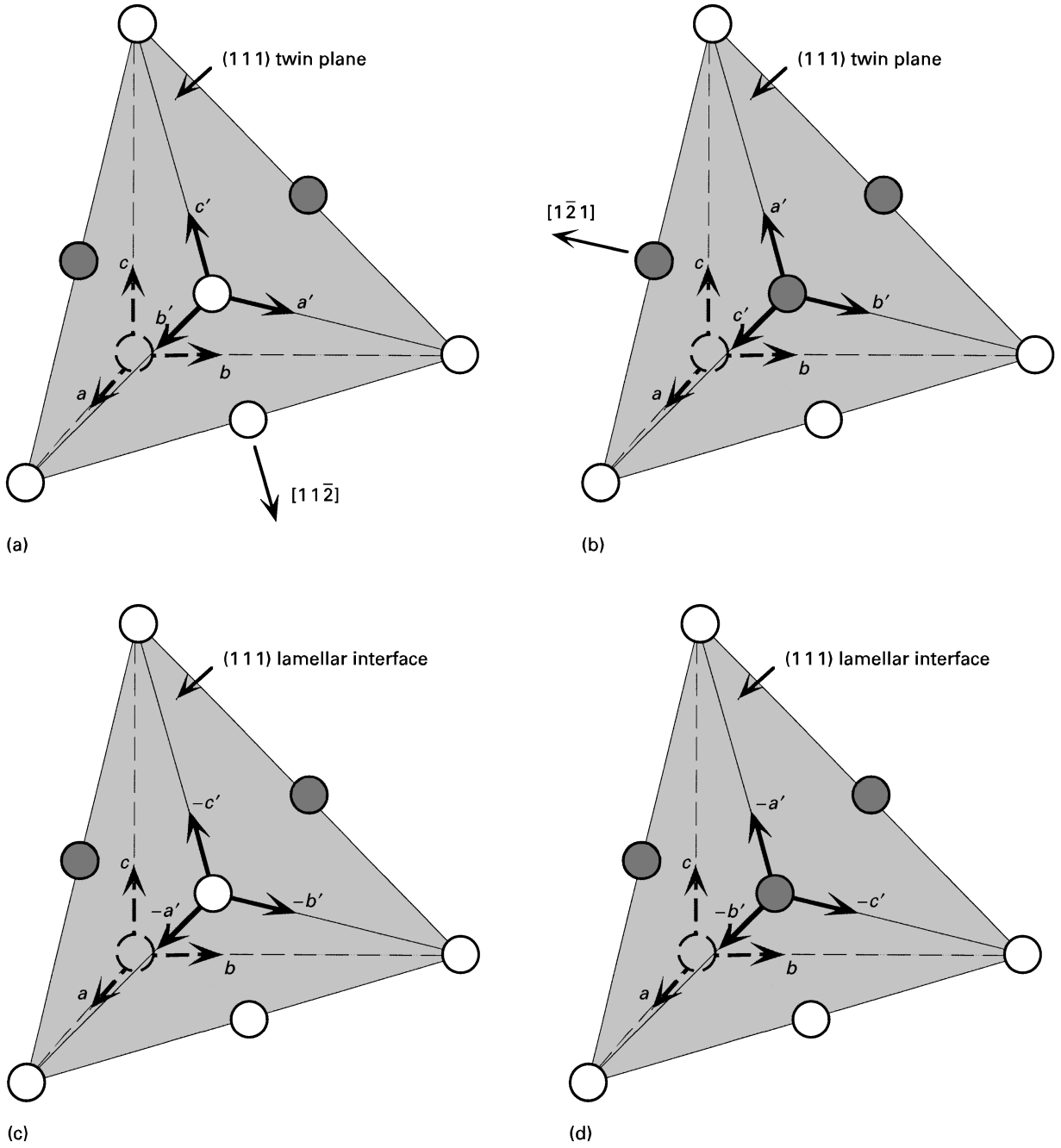

Figure 2 Four twin orientation relationships in TiAl. (a) Orientation relationship between a true-twin and the matrix; (b) orientation relationship between a pseudo-twin and the matrix; (c) orientation relationship between two true-twin-related lamellar laths; (d) orientation relationship between two pseudo-twin-related lamellar laths. In the figure, the plain letters represent the matrix crystal coordinates while those with a prime stand for the twin crystal coordinates. The shaded planes in the figure represent (1 1 1) twin planes and lamellar interfaces, so the matrix is located below the shaded plane and the twin is above the plane in each figure. The shaded and open circles represent Ti and Al atoms, respectively.

$\{\bar{1}\,1\,0\}$ projection plane and squares stand for the atoms located in the same $\{\bar{1}\,1\,0\}$ plane but above the projection plane by an $\{\bar{1}\,1\,0\}$ interplanar spacing of $(2^{1/2}/4)a$. The open and shaded marks represent Ti and Al atoms, respectively. The circled crosses indicate the projection directions in terms of the twin and the matrix as indicated in the figure. To facilitate visualization of the relative crystal orientation relationships across the twin planes or lamellar interfaces, some specific crystal planes and directions are also indexed in the figure. Atoms lying at the twin planes and the lamellar interfaces are all projected from the bottom crystals. Fig. 3a–c are the projections of the atomic arrangements across a true-twin plane, Fig. 3d–f are those across a pseudo-twin plane, Fig. 3g–i are across a true-twin related lamellar interface, and Fig. 3j–l are across a pseudo-twin related lamellar interface.

In Fig. 3a–c, we can see that atoms in the twin are all symmetric to atoms in the matrix not only in their lattice positions but also in their atomic species, which is consistent with the definition of a true-twin [12]. Although atoms at the twin plane are drawn from the bottom (matrix) crystal, these atoms do not violate the atomic arrangement of the upper (twin) crystal at the twin plane. This indicates that the interface energy of

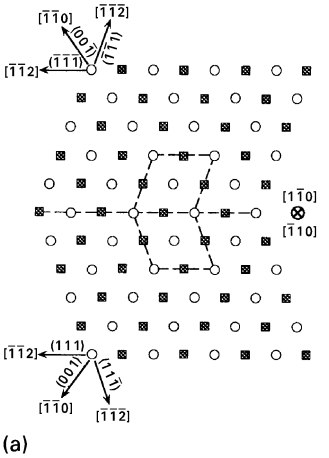

(a)

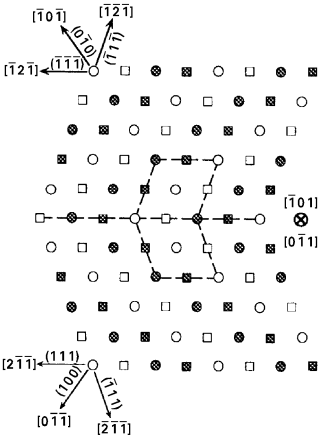

(b)

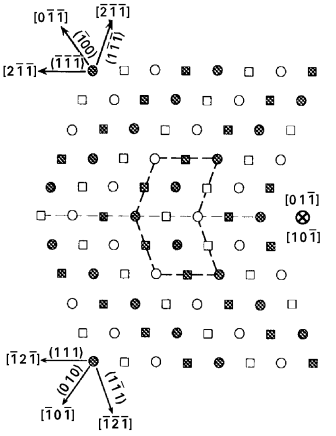

(c)

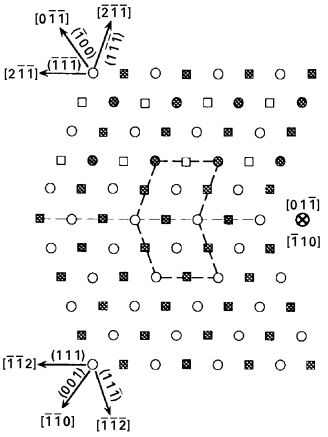

(d)

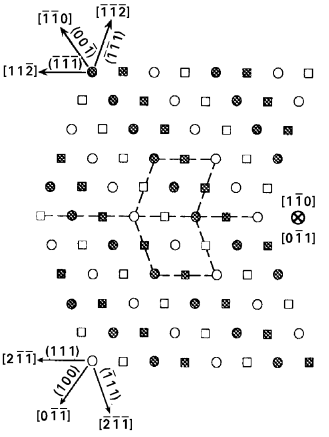

(e)

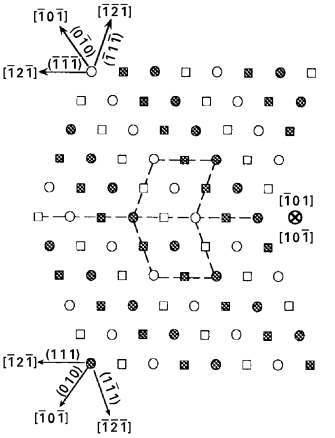

(f)

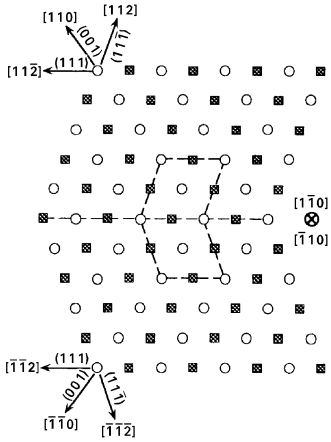

(g)

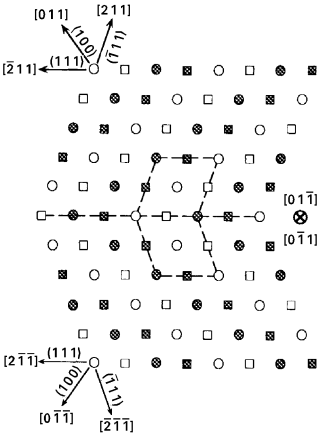

(h)

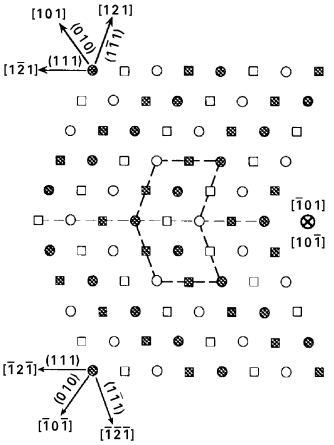

(i)

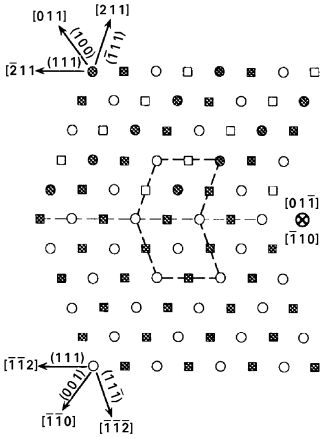

(j)

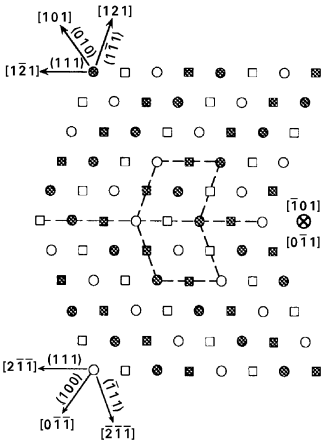

(k)

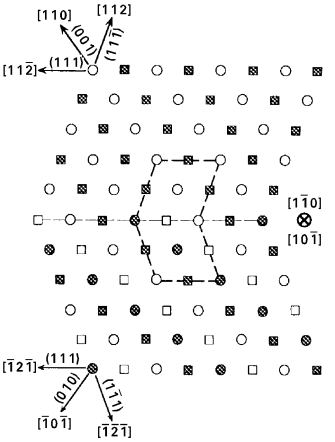

(l)

a true-twin plane should be relatively small. Since this twin is 180°-[1 1 $\bar{2}$] rotationally symmetric to the matrix, the twin plane indexes in terms of the twin and the matrix are reflected about the twin plane in all three projections. For instance, the (1 1 1) twin plane in terms of the matrix becomes the ($\bar{1}$ $\bar{1}$ $\bar{1}$) plane in terms of the twin, as shown in Fig. 3a. For other planes and directions, the reflection symmetry between the matrix and the twin is maintained only in projections along $\langle\bar{1}\,1\,0]$ directions, which is perpendicular to the [1 1 $\bar{2}$] twinning direction, as shown in Fig. 3a. The projections in directions other than $\langle\bar{1}\,1\,0]$ do not have the same reflection symmetry between the matrix and the twin in their plane and direction indexes, as shown in Fig. 3b and c.

For the pseudo-twin as shown in Fig. 3d–f, atoms in the twin are not symmetric to the same atoms in the matrix about the twin plane. In Fig. 3e and f, atoms in every second (1 1 1) plane in the twin are a reflection of the same atoms in the matrix about the twin plane. However, in Fig. 3d, atoms in the first, the third and the fifth planes of the twin are symmetric to the same atoms in the matrix about the twin plane while atoms in every second plane in the twin are symmetric to different atomic species in the matrix. This result indicates that the (1 1 1) planes in the twin and the matrix are all non-symmetric in their atomic species for pseudo-twins. Similar to the true-twin, the crystal planes and directions in the twin and the matrix are reflectionally symmetric about the twin plane only in the [1 0 $\bar{1}$]//[$\bar{1}$ 0 1] projection, as shown in Fig. 3f, which is perpendicular to the twinning direction [1 $\bar{2}$ 1]. The crystal planes and directions in the other two projections, as shown in Fig. 3d and e, are not symmetric to each other about the twin plane due to the unidirectional shear of the twinning. Atoms at the twin plane in Fig. 3d violate the atomic ordering of the twin at the twin plane but twin plane atoms in Fig. 3e and f maintain the atomic ordering of the twin at the same twin plane. This indicates that the interface energy of the pseudo-twin plane should be larger than that of a true-twin plane although the difference might not be large because the violation of atomic ordering at the pseudo-twin plane occurs only in one [$\bar{1}$ 1 0]//[0 1 $\bar{1}$] projection. However, the activation energy for pseudo-twinning should be significantly different than the activation energy of true-twinning since pseudo-twinning involves a crystal structure change from the matrix $L1_0$ to the twin $L1_1$ crystal structure as shown in Fig. 1b. Thus, the formation driving force of pseudo-twinning in γ-TiAl should be primarily determined by the formation energy of the $L1_1$ TiAl crystal structure rather than the pseudo-twin plane energy.

For the true-twin-related lamellar interface, as shown in Fig. 3g–i, the atomic arrangements across the interface are the same as those across a true-twin plane as shown in Fig. 3a–c. This suggests that the interface energy between the true-twin plane and the true-twin-related lamellar interface should be similar. However, the indexes of the planes and directions should be different between the true-twin and the true-twin-related lamellar lath with respect to the same matrix orientation. Because the true-twin-related lamellar interface is formed by a 180°-[1 1 1] rotation, the index of the lamellar interface should be (1 1 1) for both laths. Unlike the true-twin, the planes and directions in both laths follow a 180°-[1 1 1] rotational relationship in all three projections, as shown in Fig. 3g–i. This indicates that the diffraction pattern indexing for the true-twin and the true-twin-related lamellae should be different, although both diffraction patterns are the same. Comparing the crystal orientations between the true-twin portions in Fig. 3a–c and the upper laths in Fig. 3g–i, we can see that a true-twin in a specific projection has a 180°-rotational relationship about the projection direction with the corresponding lamellar lath having the same projection direction. For instance, the crystal orientation of the true-twin in Fig. 3b is exactly a 180° rotation of the upper lath in Fig. 3i about the [$\bar{1}$ 0 1] projection direction. Thus, the indexes of planes and directions of the true-twin shown in Fig. 3a–c are opposite to the corresponding planes and directions in the upper lath in Fig. 3g–i. The bottom crystal orientations are the same for all four twin relationships shown in Fig. 3 in order to compare the crystal orientation differences between twins and laths.

Unlike the relationship between a true-twin and a true-twin-related lamella, the pseudo-twin-related lamellar lath has a completely different atomic arrangement from the pseudo-twin. In a pseudo-twin-related lamellar lath, the anti-atomic symmetry (an atom is symmetric to a different atom) across the interface exists in every (1 1 1) plane in all projections, as shown in Fig. 3j–l. This difference in atomic arrangement across the pseudo-twin plane and the pseudo-twin-related lamellar interface is not surprising given that the two crystal structures are different. However, the indexes of the planes and directions in the two crystals in the same projection direction, for instance the [1 $\bar{1}$ 0] projection direction as shown in Fig. 3e and l, also have 180°-rotational relationships about the projection direction, similar to that between the true-twin and the true-twin-related lamellar lath. Investigating the atomic arrangements at the lamellar interface shown in Fig. 3j–l, the interface atomic violation at the pseudo-twin-related lamellar interface is seen to occur in more projections compared to that for the pseudo-twin plane. Atoms at the pseudo-twin-related lamellar interface violate the atomic ordering of the upper crystal in all three projections, as seen in Fig. 3j–l, while in the pseudo-twin plane case the violation occurs only in one projection, as in Fig. 3d.

Figure 3 Atomic arrangements across the twin planes and the twin-related lamellar interfaces as viewed along $\langle\bar{1}\,1\,0\rangle$ directions. (a)–(c) are atomic arrangements across the true-twin plane, (d)–(f) are across the pseudo-twin plane, (g)–(i) are across the true-twin-related lamellar interface, and (j)–(l) are across the pseudo-twin-related lamellar interface. Circles represent the atoms in $\{\bar{1}\,1\,0\}$ projection planes and squares represent the atoms in the same $\{\bar{1}\,1\,0\}$ planes but above the projection plane by an interplanar spacing. The shaded and open marks are Ti and Al atoms, respectively. Atoms at the interfaces belong to the bottom crystals. The circled crosses indicate the projection directions in terms of the twin and the matrix.

Thus, if we consider only the interface atomic violation effect on the interfacial energy, the pseudo-twin-related lamellar interface should have a higher interfacial energy than a pseudo-twin plane. Based on this argument, the low occurrence of pseudo-twinning in γ-TiAl crystals may be ascribed to the structural changes in pseudo-twinning rather than the pseudo-twin plane energy. Since pseudo-twin-related lamellae are related by a 60°-rotation about the lamellar interface normal, we cannot see the reflection orientation relationship between the upper and bottom crystals in terms of their crystal plane or direction indexes.

4. Identification of true-twin and pseudo-twin relationships

In this section, we will analyse the diffraction patterns from both types of deformation twins and twin-related lamellae in order to identify the true-twin and pseudo-twin relationships among the deformation twins and twin-related lamellae. The diffraction patterns for all four twin relationships are simulated by considering the structure factors, angles between planes, and through comparison with the experimentally obtained diffraction patterns [11]. The simulated $\langle \bar{1}\,1\,0 \rangle$ zone diffraction patterns with respect to the crystal orientations presented in Fig. 3 are shown in Fig. 4. All the diffraction patterns shown in Fig. 4 were obtained parallel to the twin planes and the lamellar interfaces. Consistent with the formation mechanisms for deformation twins and lamellar structures, the diffraction patterns are indexed in such a way that the diffraction patterns are reflectionally symmetric about the plane perpendicular to the $\mathbf{g} = [1\,1\,1]$ vector (i.e. the (1 1 1) plane) for deformation twins and 180°-rotationally symmetric about the $\mathbf{g} = [1\,1\,1]$ vector for lamellae. In diffraction patterns for the twin-related lamellae, one lath is assumed to be the matrix (the bottom lath in Fig. 3) and the other is assumed to be the twin consistent with the diffraction patterns of the deformation twins.

For true-twin diffraction patterns as shown in Fig. 4a–c, superlattice diffraction spots may or may not be seen from both the twin and the matrix in a diffraction pattern. Comparing these diffraction patterns with the diffraction patterns from a true-twin-

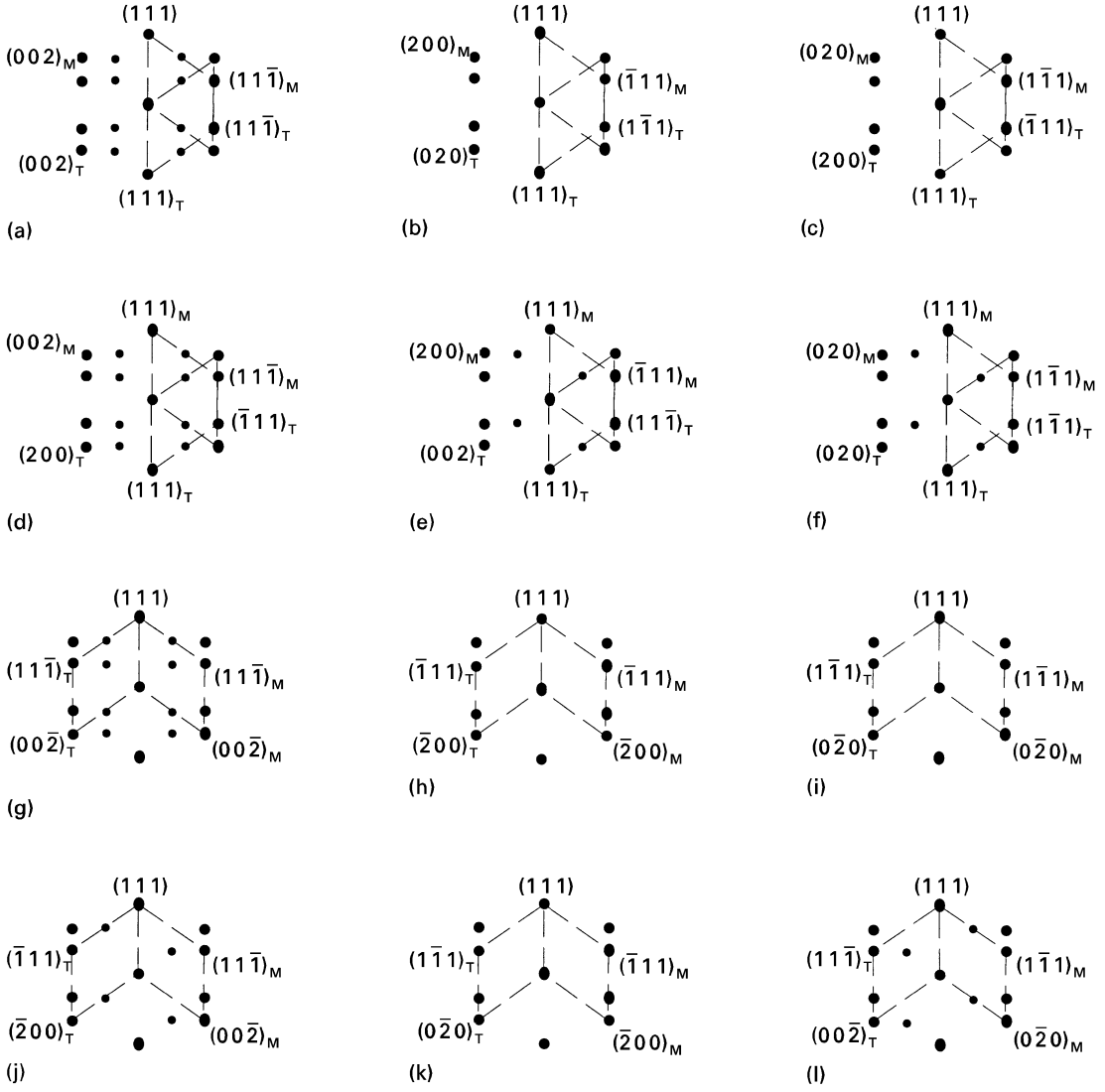

Figure 4 Simulated $\langle \bar{1}\,1\,0 \rangle$ zone diffraction patterns across (a)–(c) the true-twin plane, (d)–(f) the pseudo-twin plane, (g)–(i) the true-twin-related lamellar interface, and (j)–(l) the pseudo-twin-related lamellar interface. Diffraction patterns are indexed based on the 180°-$\langle 1\,1\,\bar{2} \rangle$ rotational symmetry for the deformation twins, the 180°-[1 1 1] rotational symmetry for the true-twin-related lamellae and the 60°-[1 1 1] rotational symmetry for the pseudo-twin-related lamellae.

TABLE I Diffraction criterion for identification of the four twin relationships in TiAl

	True-twin	Pseudo-twin	True-twin lamellae	Pseudo-twin lamellae
True-twin		$\langle 1\,0\,\bar{1}\rangle_M$	Morphology	$\langle\bar{1}\,1\,0]$
Pseudo-twin	$\langle 1\,0\,\bar{1}\rangle_M$		$\langle 1\,0\,\bar{1}\rangle_M$	$\langle 0\,\bar{1}\,1\rangle_M//\langle\bar{1}\,0\,1]_T$ $\langle\bar{1}\,1\,0]_M$
True-twin lamellae	Morphology	$\langle 1\,0\,\bar{1}\rangle_M$		$\langle\bar{1}\,1\,0]$
Pseudo-twin lamellae	$\langle\bar{1}\,1\,0]$	$\langle 0\,\bar{1}\,1\rangle_M//\langle\bar{1}\,0\,1]_T$ $\langle\bar{1}\,1\,0]_M$	$\langle\bar{1}\,1\,0]$	

related lamella as shown in Fig. 4g–i, we can see that these two sets of diffraction patterns do not differ in their configurations except for the exact diffraction spot indexes. Accordingly, based solely on the diffraction patterns we cannot distinguish a true-twin from a true-twin-related lamella. The only remaining possibility of distinguishing between them is by their morphologies and by comparing their microstructures before and after deformation.

For pseudo-twin diffraction patterns as shown in Fig. 4d–f, the superlattice spots from the twin occur in all three zone diffraction patterns due to the $L1_1$ crystal structure of the pseudo-twin. The superlattice spots from the matrix are only evident in the $[\bar{1}\,1\,0]_M$ zone diffraction pattern. Comparing the pseudo-twin diffraction patterns with the true-twin diffraction patterns, we can see that the diffraction patterns in Fig. 4a and d are similar. Therefore, these patterns cannot be used to distinguish between a true-twin and a pseudo-twin. To distinguish between the two deformation twins, we must use $\langle\bar{1}\,0\,1]_M$ zone diffraction patterns, as shown in Fig. 4b c, e and f. The same $\langle\bar{1}\,0\,1]_M$ zone diffraction patterns, should be applied to distinguish a pseudo-twin from a true-twin-related lamella.

Comparing the diffraction patterns for a pseudo-twin-related lamella in Fig. 4j–l with those of a true-twin in Fig. 4a–c or those of a true-twin-related lamella in Fig. 4g–i, the $[0\,\bar{1}\,1]_M$ zone diffraction pattern in Fig. 4k also shows no superlattice diffraction spots from both crystals, as in Fig. 4b, c, h and i. Thus to distinguish a pseudo-twin-related lamella from a true-twin and a true-twin-related lamella, only $\langle\bar{1}\,1\,0]_M$ zone diffraction patterns are useful. To distinguish a pseudo-twin-related lamella from a pseudo-twin, diffraction patterns from the $\langle 0\,\bar{1}\,1\rangle_M//\langle\bar{1}\,0\,1]_T$ zones for a pseudo-twin-related lamella and $\langle\bar{1}\,1\,0]_M$ zone diffraction patterns for a pseudo-twin should be used.

The diffraction identification criterion among the four twin relationships in γ-TiAl is summarized in Table I.

5. Conclusions

The four twin relationships in γ-TiAl have been crystallographically studied. Based upon this analysis, the following conclusions can be drawn:

1. Crystal orientations between deformation twins and the matrix in TiAl are 180°-rotationally symmetric about the twinning direction $\langle 1\,1\,\bar{2}\rangle$. Contrarily, the crystal orientations between two twin-related lamellar laths are related by a 180°-rotational symmetry about the lamellar interface normal [1 1 1].

2. Atomic arrangements across a true-twin plane and a true-twin-related lamellar interface are similar, but the atomic arrangements across a pseudo-twin plane and a pseudo-twin-related lamellar interface are quite different. This is due to the structural change from $L1_0$ to $L1_1$ upon pseudo-twinning. Atoms at the true-twin plane and the true-twin-related lamellar interface do not violate the atomic order in both crystals while those at a pseudo-twin plane and a pseudo-twin-related lamellar interface violate the atomic order.

3. The true-twin and true-twin-related lamellae cannot be distinguished between using $\langle\bar{1}\,1\,0\rangle$ zone diffraction patterns. Similarly, not every $\langle\bar{1}\,1\,0\rangle$ zone diffraction pattern is sufficient to distinguish between any two different twin relationships. A true-twin and a pseudo-twin can be distinguished only by using $\langle 1\,0\,\bar{1}]$ zone diffraction patterns, while a true-twin and a pseudo-twin-related lamellae can be distinguishable only by using $\langle\bar{1}\,1\,0]$ zone diffraction patterns.

Acknowledgement

This research was conducted under the auspices of the US Department of Energy.

References

1. H. INUI, M. H. OH, A. NAKAMURA and M. YAMAGUCHI, *Phil. Mag. A.* **66** (1992) 539.
2. Y.-W. KIM, *Acta Metall.* **40** (1992) 1121.
3. S. FARENC, A. COUJOU and A. COURET, *Phil. Mag. A* **67** (1993) 127.
4. Z. JIN and T. R. BIELER, *ibid.* **71** (1995) 925.
5. S. M. L. SASTRY and H. A. LIPSITT, *Met. Trans. A* **8A** (1977) 299.
6. H. INUI, A. NAKAMURA, M. H. OH and M. YAMAGUCHI, *Phil. Mag. A* **66** (1992) 1557.
7. Z. JIN, R. BEALS and T. R. BIELER, in "Structural intermetallics", edited by R. Darolia, J. J. Lewandowski, C. T. Liu, P. L. Martin, D. B. Miracle and M. V. Nathal (TMS, Warrendale, PA, 1993) p. 275.
8. G. T. GRAY III, in "Twinning in advanced materials", edited by M. Y. Yoo and M. Wuttig (TMS, Warrendale, PA, 1994) p. 337.
9. M. A. MORRIS, *Phil. Mag. A* **69** (1994) 129.
10. S. A. MALOY and G. T. GRAY III, *Acta Metall.* **44** (1996) 1741.
11. Z. JIN and G. T. GRAY III, *Mater. Sci. Eng.* A23 (1997) 62.
12. J. W. CHRISTIAN and D. E. LAUGHLIN, *Acta Metall.* **36** (1988) 1617.

Received 30 September 1996
and accepted 9 May 1997